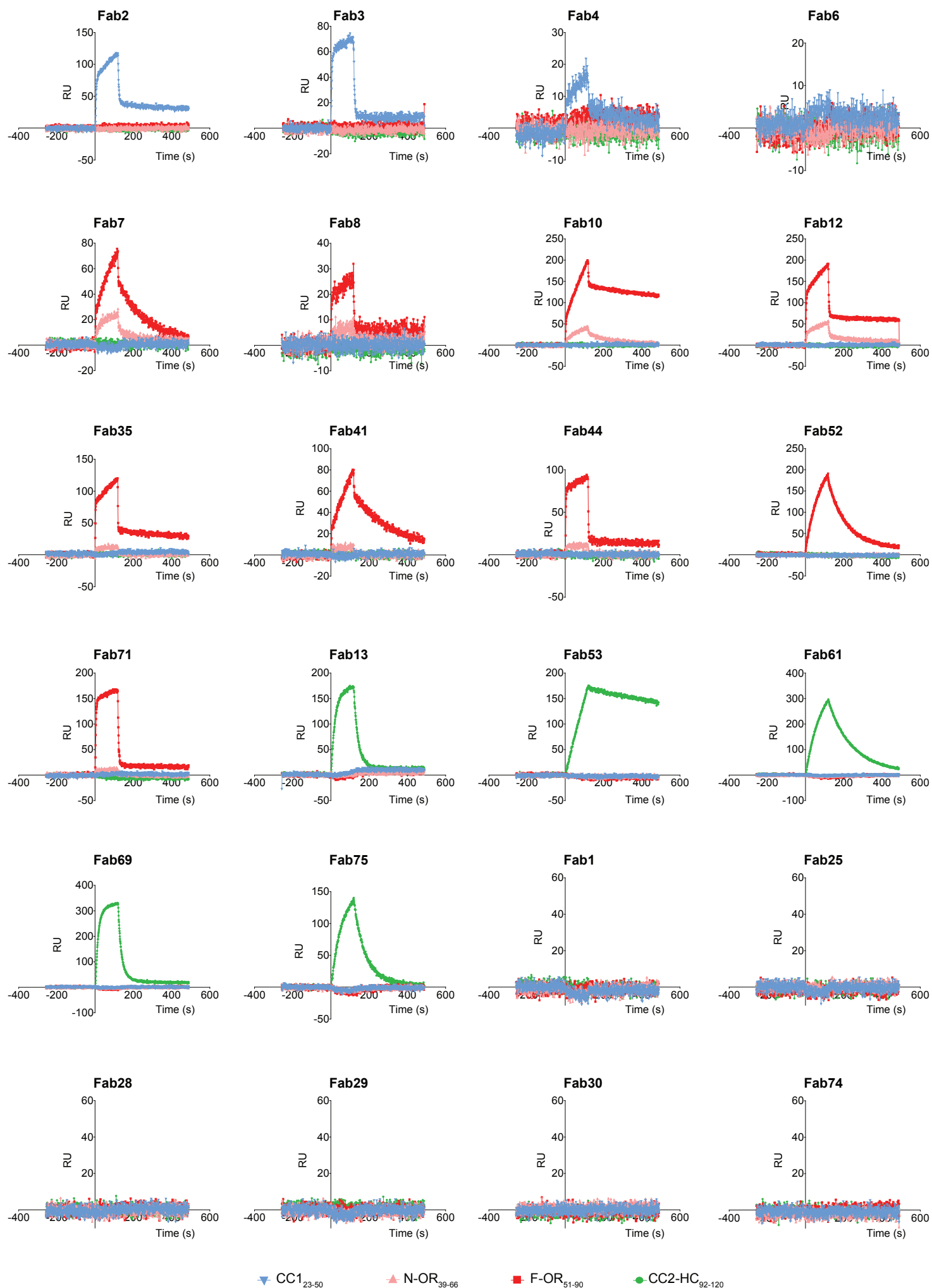
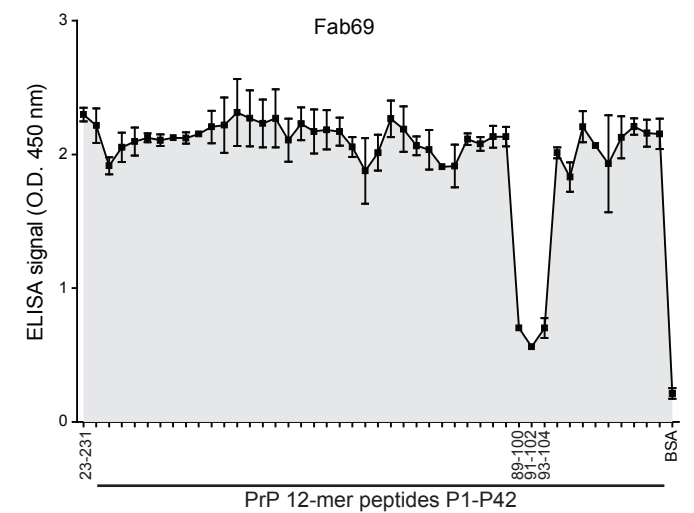
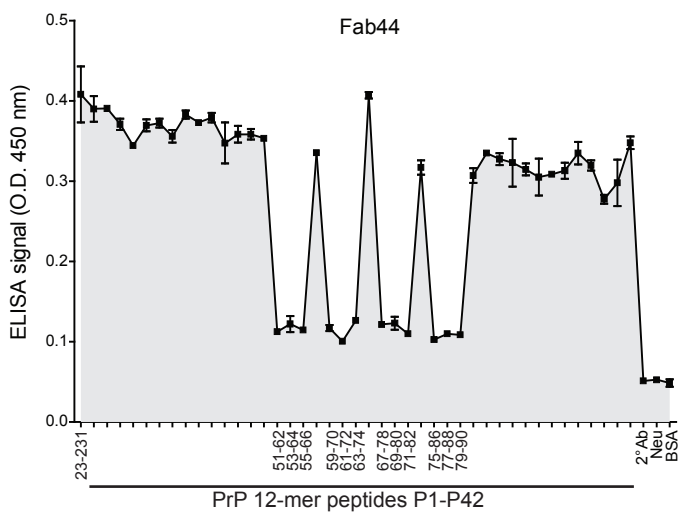
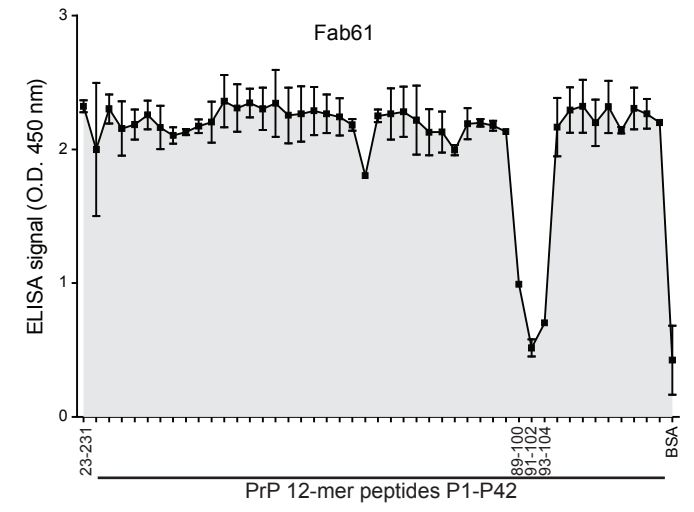
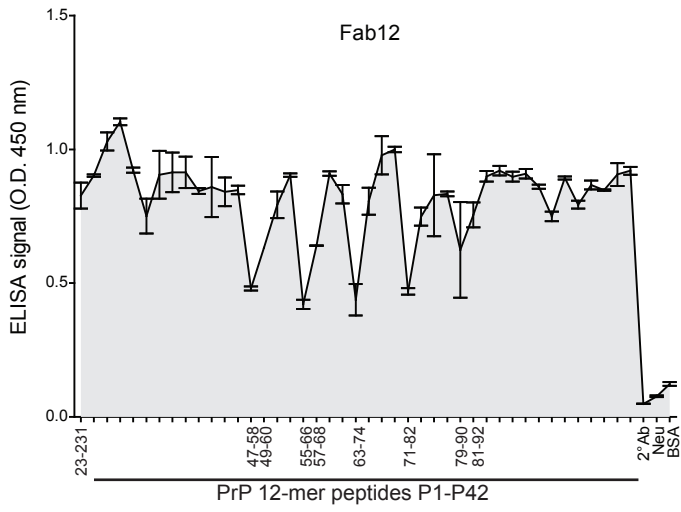
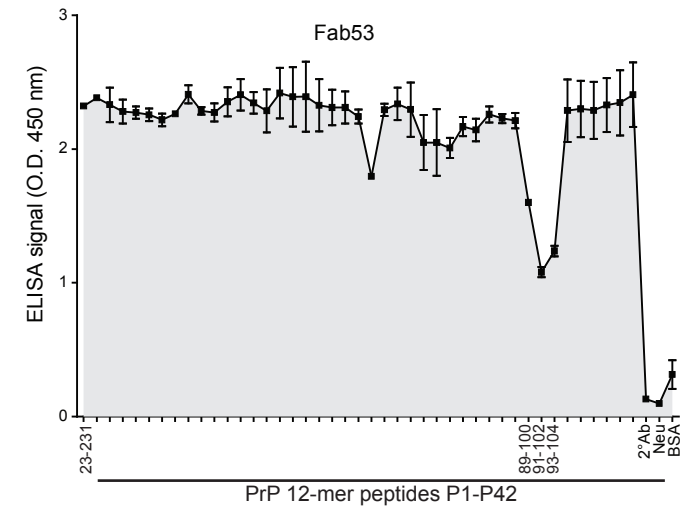
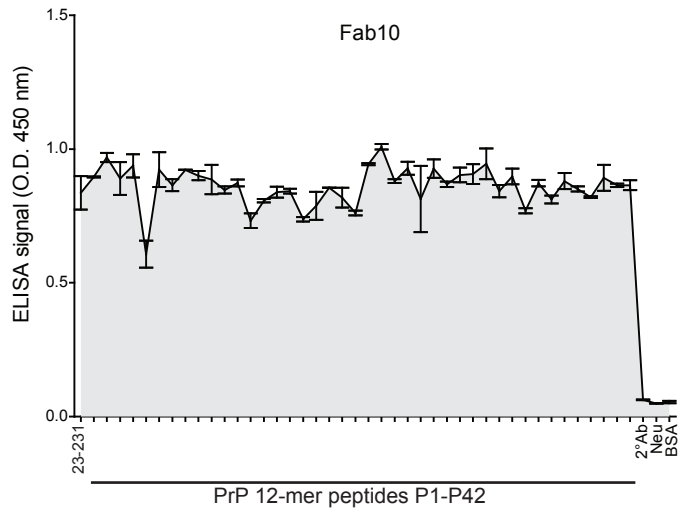
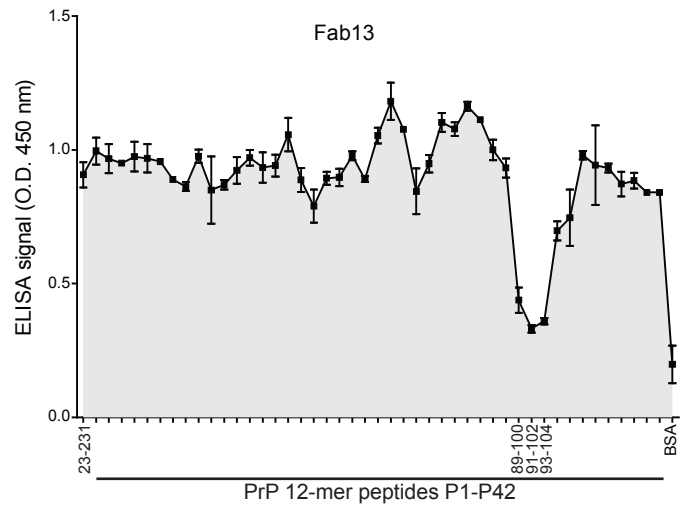
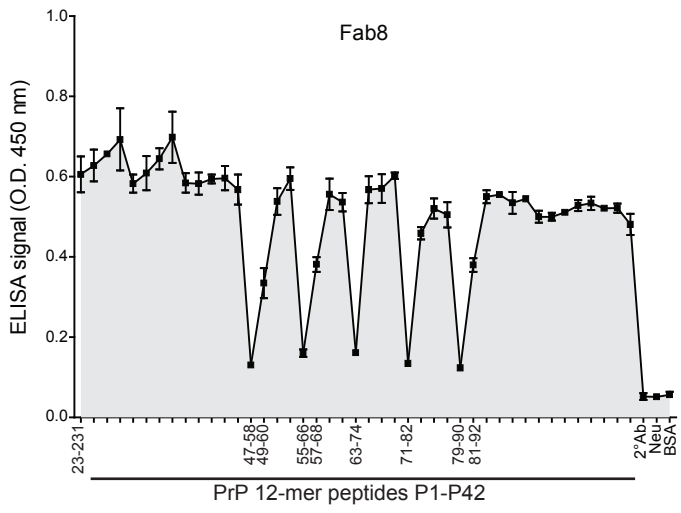


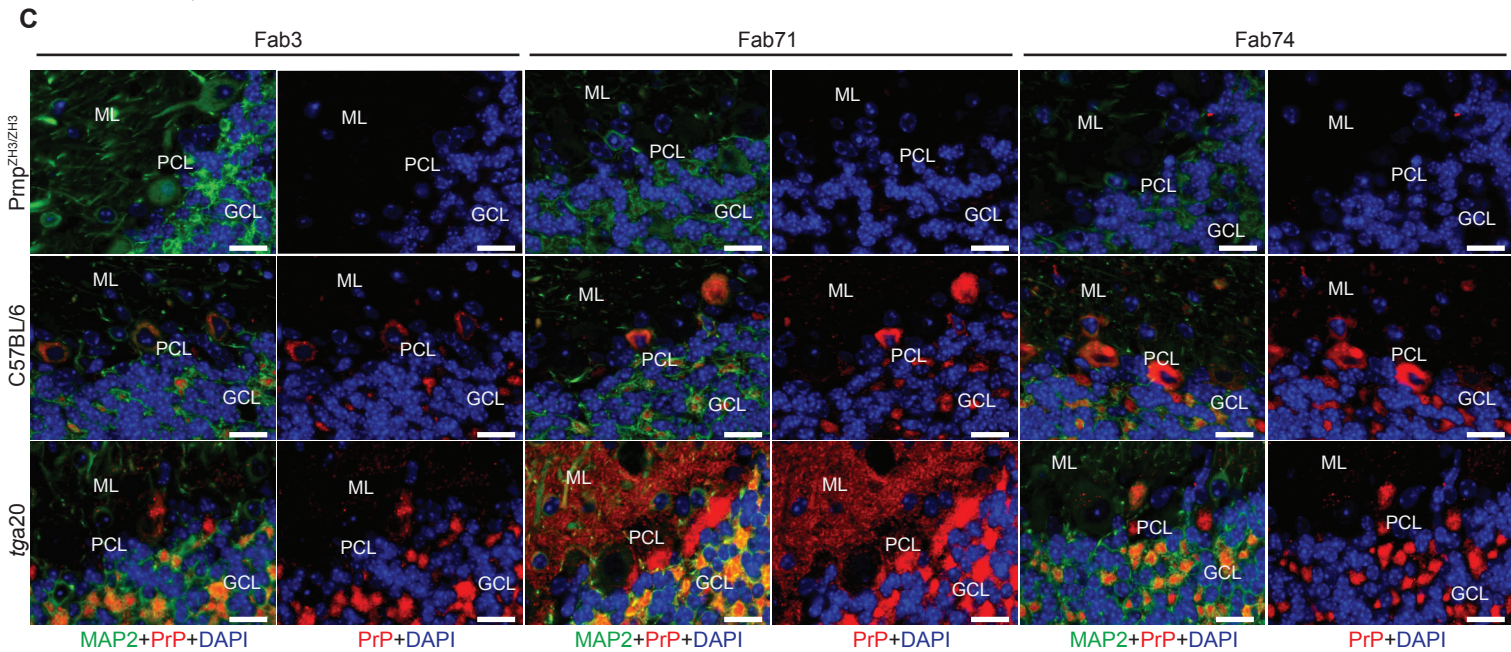
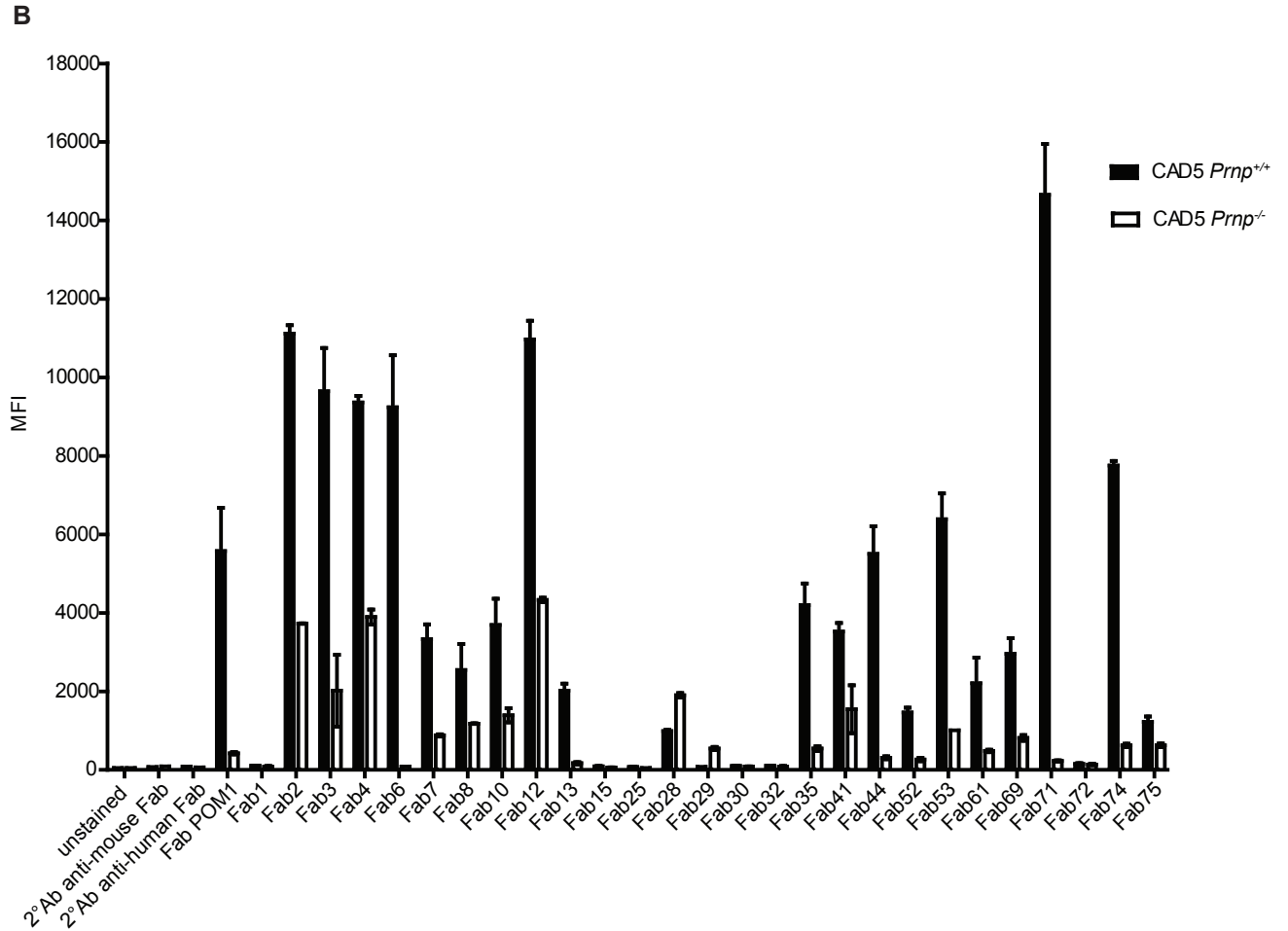
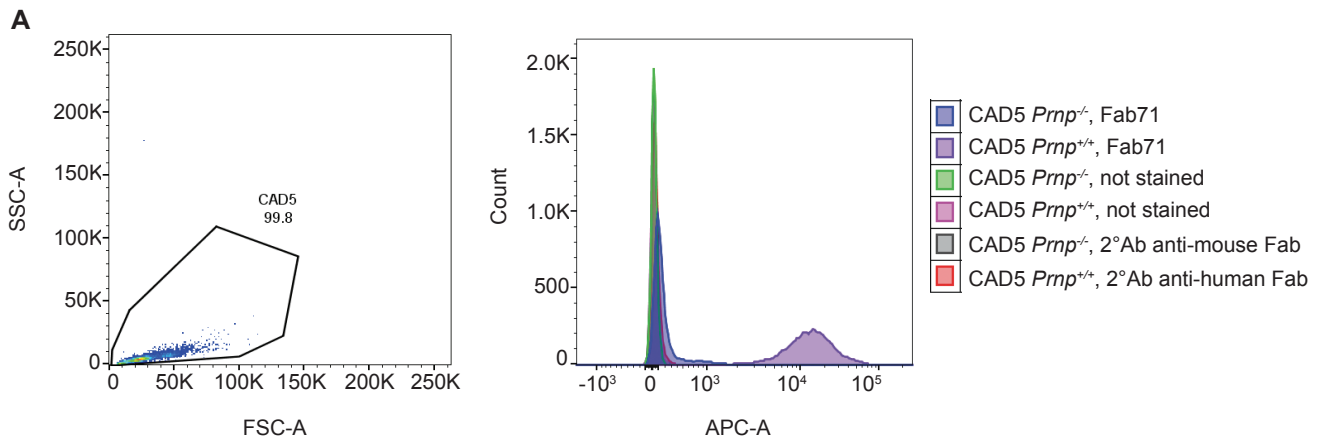
Appendix information

Table of content:

- 1. Appendix Figure S1**
- 2. Appendix Figure S2**
- 3. Appendix Figure S3**
- 4. Appendix Figure S4**
- 5. Appendix Figure legends**
- 6. Appendix Table S1**
- 7. Appendix Table S2**
- 8. Appendix Table S3**
- 9. Appendix Table S4**
- 10. Appendix Table S5**
- 11. Appendix Table S6 (exact p-values)**

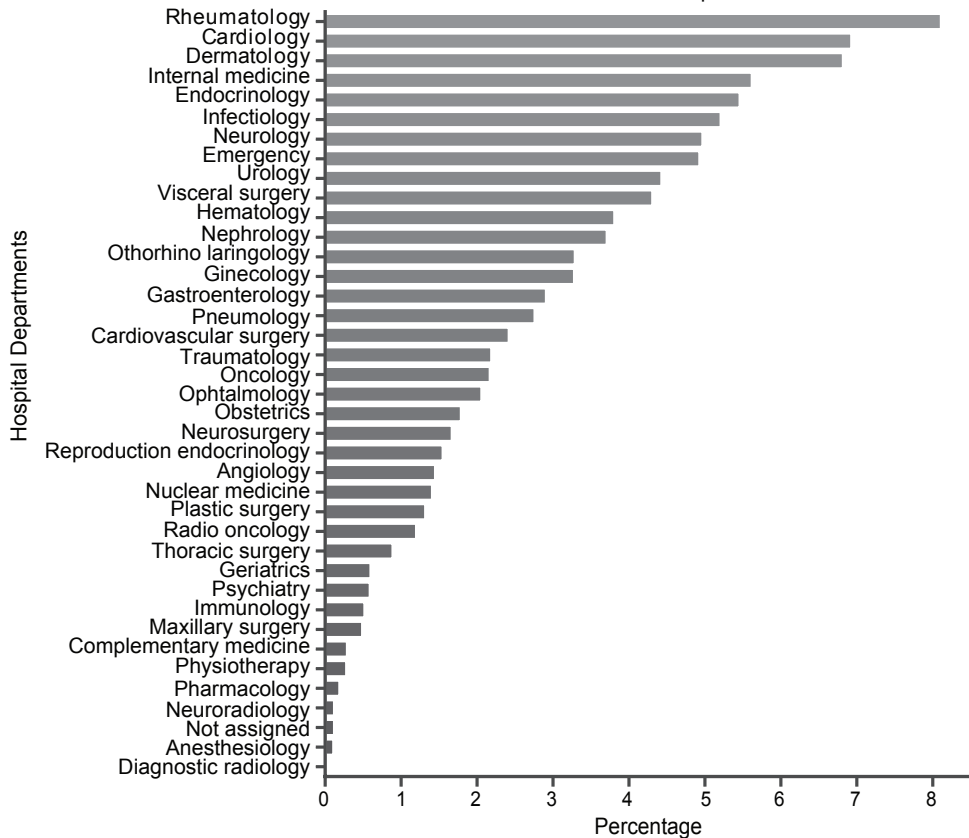




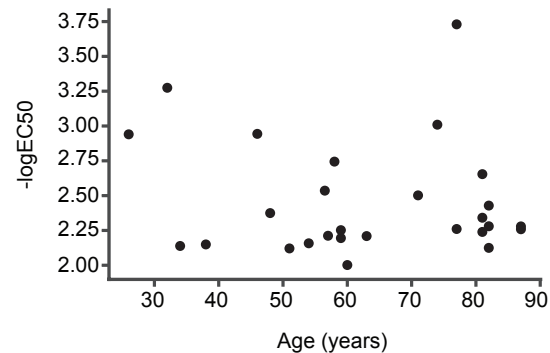


A

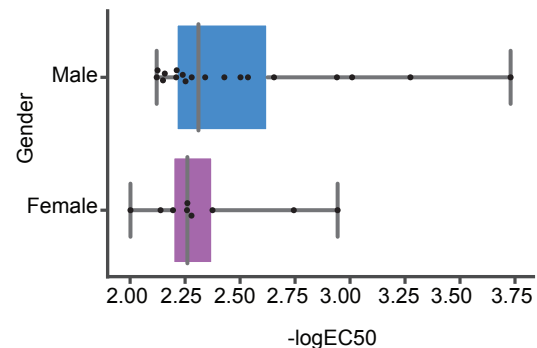
Source of all samples

**B**

-logEC50 versus age of all hits

**C**

-logEC50 distribution of hit males and females



Appendix figure legends

Appendix Fig. S1: Epitope confirmation by SPR. Biotinylated PrP peptides were immobilized on an NLC sensor chip and the binding of the indicated Fabs was measured by SPR. Epitope assessment by SPR confirmed the results obtained by ELISA. RU: relative units.

Appendix Fig. S2: Epitope mapping by competition ELISA. FT-competition ELISA to map the epitopes of the OR₅₁₋₉₁ binders (Fab8, Fab10, Fab44, Fab12) and CC2-HC₉₂₋₁₂₀ binders (Fab13, Fab53, Fab61, Fab69). Peptides that strongly inhibit the binding of the Fabs to recPrP₂₃₋₂₃₁ are indicated by their residue numbers in the PrP sequence and reflect the respective binding epitopes. Positive control: recPrP₂₃₋₂₃₁. Negative controls: Neu, BSA, and 2° Ab.

Data information: ELISA data were performed in duplicates. Data represent the mean ± sem.

Appendix Fig. S3: Anti-PrP Fabs detect cell surface exposed wtPrP^C and stain wtPrP^C in paraffin embedded mouse brain sections.

(A) Flow cytometry analysis of the Fabs compared to Fab-POM1 used as positive control for the staining. CAD5 *Prnp*^{+/+} and *Prnp*^{-/-} cells were incubated with the Fabs at 150 µg/ml, and analyzed with an APC-labelled anti-human Fab antibody. Representative flow cytometry dot plot of FSC-A (forward scatter)/SSC-A (side scatter) of CAD5 *Prnp*^{+/+} stained with Fab71 (left) and fluorescence intensity plot of CAD5 *Prnp*^{+/+} and *Prnp*^{-/-} cells.

(B) Bar graph showing the average mean fluorescent intensity (MFI) for each Fab. Increased MFIs indicate binding of the Fabs to wtPrP^C on the cell surface. Each Fab was tested in duplicate.

Data information: Data represent the mean ± sem.

(C) Immunofluorescent staining of cerebellar brain sections of *Prnp*^{ZH3/ZH3}, wt and *tga20* mice with either Fab3, Fab71, or Fab74 (displayed in red). Anti-MAP2 antibody (microtubule-associated protein 2) was used as neuronal marker (in green) and DAPI to stain the cell nuclei

(in blue). The Fabs detected wtPrP^C in the cerebellar granule cell layer (CGL) and molecular layer (ML) of wt and *tga20* mice. As expected, the Fabs did not detect wtPrP^C in Purkinje cell layer (PCL) of *tga20* mice. The higher staining intensity of Fab71 might be caused by its ability to recognize the repetitive epitopes within the OR multiple times. Scale bar: 20 μ m.

Appendix Fig. S4: Medical and demographic data of the hospital cohort screened for anti-PrP antibodies and of the hits identified in the primary screening.

(A) Bar plot indicating the hospital departments from which the tested 37,894 samples were obtained.

(B,C) Correlations between $-\log(\text{EC50})$ and age (B), $-\log(\text{EC50})$ and sex (C). Black dots in panels (B) and (C) indicate each of the 27 hits that were identified in the primary screen.

Data information: The boxplot divides the data set into three quartiles. The box extends from the first to the third quartile values of the data set, with a line at the median. The whiskers extend from the box to show the range of the data (minimum and maximum).

Appendix Table S1: Matrix of the different washing conditions during panning

Washing time	A1 (standard)	A2 (high salt)	A3 (detergent)
5 times quick, 10 times 5 min	PBST	PBST + 1M NaCl	PBS + 2% Octyl β -D-glucopyranoside
5 times quick, 7 times 5 min	PBS	PBS + 1M NaCl	PBS + 2% Octyl β -D-glucopyranoside
3 times 5 min	PBS	PBS	PBS

Appendix Table S2: Criteria for sorting the NGS counts for epitope prediction of the anti-PrP Fabs

Panning output NGS libraries															
mouse PrP amino acid residues	PrP domains		Ref	binding strength		synthetic biotinylated PrP peptides					recombinant PrP fragments			negative controls	
				recPrP ₂₃₋₂₃₁	recPrP ₂₃₋₂₃₁ high salt	recPrP ₂₃₋₂₃₁ detergent	CC1 ₂₃₋₅₀ SP	CC1 ₂₃₋₅₀ LP	N-OR ₃₉₋₆₆	F-OR ₅₁₋₉₁	CC2-HC ₉₂₋₁₂₀	recPrP ₂₃₋₁₁₀	recPrP ₉₀₋₂₃₁	recPrP ₁₂₁₋₂₃₁	Neutravidin
23-38	CC1	CC1_SP	1	ns	ns	>0	ns	0	0	0	>0	0	0	0	0
		CC1_LP	1	ns	ns	ns	>0	0	0	0	>0	0	0	0	0
39-50	CC1-N-OR		1	ns	ns	ns	ns	>0	0	0	>0	0	0	0	0
50-66	N-OR		1	ns	ns	0	0	>0	ns	0	>0	0	0	0	0
51-91	F-OR		1	ns	ns	0	0	ns	>0	0	>0	0	0	0	0
92-110	CC2-HC		1	ns	ns	0	0	0	0	>0	>0	>0	0	0	0
111-120	CC2-HC		1	ns	ns	0	0	0	0	>0	0	>0	0	0	0
90-231	CC2-GD		1	ns	ns	0	0	0	0	0	0	>0	>0	0	0
121-231	GD		1	ns	ns	0	0	0	0	0	0	0	>0	0	0

Ref: reference panning to recPrP₂₃₋₂₃₁

CC1_SP: CC1 Solid Phase

CC1_LP: CC1 Liquid Phase

ns: not selected

Appendix Table S3: EC₅₀ of Fab3 and Fab71 and their respective affinity matured variants as determined by ELISA

	EC₅₀ (nM)	R square
Fab3	30.430	0.965
Fab81	0.184	0.987
Fab82	0.298	0.984
Fab83	0.044	0.982
Fab84	0.530	0.990
Fab85	0.465	0.989
Fab86	0.541	0.981
Fab87	0.385	0.991
Fab88	0.474	0.989
Fab89	0.421	0.993
Fab90	0.235	0.961
Fab91	0.450	0.984
Fab92	0.260	0.992
Fab93	0.518	0.989
Fab94	0.210	0.992
Fab95	0.511	0.994
Fab96	1.516	0.987
Fab97	0.322	0.977
Fab98	1.005	0.990
Fab99	1.119	0.995

	EC₅₀ (nM)	R square
Fab71	24.890	0.992
Fab100	0.232	0.983
Fab101	0.190	0.964
Fab102	0.238	0.981
Fab103	0.266	0.976
Fab104	0.380	0.958

Appendix Table S4: Features and clinical data of the subjects displaying high titre of anti-PrP autoantibodies in the plasma.

Patient ID	Core diagnoses	Sex	Year of birth
Patient_01	Valvular and coronary heart disease; chronic obstructive pulmonary disease	Male	1943
Patient_02	Contusion of digit	Female	1971
Patient_03	Chronic lymphatic leukaemia; valvular cardiac disease; chronic kidney insufficiency; oncocytoma	Male	1937
Patient_04	Not shown		
Patient_05	Myeloid leukaemia	Male	1959
Patient_06	Aortic stenosis	Male	1947
Patient_07	Not shown		
Patient_08	Aortic aneurysm and dissection	Male	1937
Patient_09	Ulcerating colitis; drug abuse	Female	1970
Patient_010	Not shown		
Patient_014	HIV infection; erectile dysfunction; gonarthrosis	Male	1959
Patient_015	Intraspinal space-consuming lesion (ganglioneurom WHO grade I); drug abuse	Male	1985
Patient_016	Coronary heart disease; severe kidney insufficiency; hypothyreosis	Female	1959
Patient_017	Polyserositis; mamma carcinoma	Female	1958
Patient_018	HIV infection	Male	1991
Patient_019	Not shown		
Patient_020	Urothel carcinoma; adenocarcinoma; arrhythmogenic cardiac disease	Male	1936
Patient_021	Coronary 2-vessel disease	Male	1954
Patient_022	Coronary heart disease; neuropathic pain	Male	1935
Patient_023	T cell lymphoma	Male	1967
Patient_024	Injury of the pelvic ring	Male	1964
Patient_025	Status epilepticus; myxofibrosarcoma; slight dementia type Alzheimer's disease	Female	1931
Patient_026	Squamos cell carcinoma	Female	1941
Patient_027	Not shown		
Patient_028	Syncope; severe depressive episodes	Female	1985
Patient_029	Not shown		
Patient_030	Adenocarcinoma; signs of dementia	Male	1937

Shown are the core diagnoses, the sex, and the year of birth for the 21 out of 27 individuals identified with autoantibodies against recombinant PrP in the high-throughput antibody profiling. We have refrained from displaying any patient-associated information from patients who do not gave expressive consent by signing the hospital-wide general consent of the University Hospital of Zurich. While many but not all of the patients included here are highly multimorbid, only the core diagnoses were selected for display, also with respect to the appropriate handling of sensitive patient data.

Appendix Table S5: Comparison of age, gender and clinical data between subjects with and without high titre PrP autoantibodies.

Median age hits	# hits	Median age non-hits	# non-hits	P-value
61	27	55	48691	3.58E-02

% male hits	% female hits	% male non-hits	% female non-hits	P-value
66.67	33.33	52.42	47.64	1.96E-01

ICD-10 code	# hits	# non-hits	# hits	# non-hits	P-value	Bonferroni
E87	6	4830	22.22	9.92	4.56E-02	1.82E-01
I25	7	6207	25.93	12.75	7.33E-02	2.93E-01
I10	9	11595	33.33	23.81	2.59E-01	1
N18	5	5874	18.52	12.06	3.76E-01	1

Statistical testing for difference in age (median test, significance at $\alpha \leq 0.01$) or gender (chi-square test, significance at $\alpha \leq 0.01$) revealed no significant difference. Analysis of enriched ICD-10 codes in patients with anti-PrP-autoantibodies versus patients without. No patterns could be discerned and no ICD-10 code reached a statistically significant enrichment (chi-square test, significance at $\alpha \leq 0.01$, Bonferroni correction for multiple comparisons).

Appendix Table S6: exact *p*-values

Figure panel	comparison	<i>p</i>-value
Figure 3C	NBH: untreated vs Fab 25	0.000683
	Prion: untreated vs Fab83	0.001199
	Prion: untreated vs Fab8	3.6E-14
	Prion: untreated vs Fab44	6.67E-12
	Prion: untreated vs Fab71	9.89E-10
	Prion: untreated vs Fab100	7.16E-10
Figure 3D	untreated vs Fab100	0.003309
Figure EV3C	CAD5-Prnp ^{-/-} non transfected vs WtPrPC	0.0001
	CAD5-Prnp ^{-/-} non transfected vs PrP Δ 23-31	0.006
	CAD5-Prnp ^{-/-} non transfected vs PrP Δ 23-27	0.0148
	CAD5-Prnp ^{-/-} non transfected vs [[PrP]] ₍₂₃₋₂₇₎ ^(K→A)	0.0001
	CAD5-Prnp ^{-/-} non transfected vs [[PrP]] ₍₂₃₋₂₇₎ ^{Mirror}	0.0025
Figure EV5A	Prion vs Prion + Fab71	0.001173
Figure EV5B	Prion vs Prion + Fab100	0.019613